IFAC Journal of Systems and Control 29 (2024) 100272

Contents lists available at ScienceDirect

IFAC Journal of Systems and Control

journal homepage: www.elsevier.com/locate/ifacsc

Full length article

Analysis on the contribution of glucagon receptors to glucose dynamics in type 1 diabetes

Clara Furió-Novejarque [a], Iván Sala-Mira [a], Ajenthen G. Ranjan [b], Kirsten Nørgaard [b], José-Luis Díez [a,d], John Bagterp Jørgensen [c], Jorge Bondia [a,d,*]

[a] Instituto Universitario de Automática e Informática Industrial, Universitat Politècnica de València, C/Camí de Vera, s/n, València, 46022, Spain
[b] Steno Diabetes Center Copenhagen, Borgmester Ib Juuls Vej 83, Herlev, 2730, Denmark
[c] Department of Applied Mathematics and Computer Science, Technical University of Denmark, Anker Engelunds Vej 1, Kgs. Lyngby, 2800, Denmark
[d] Centro de Investigación Biomédica en Red de Diabetes y Enfermedades Metabólicas Asociadas, Instituto de Salud Carlos III, Av. Monforte de Lemos 3-5, Madrid, Spain

ARTICLE INFO

Article history:
Received 13 October 2023
Received in revised form 3 June 2024
Accepted 18 June 2024
Available online 24 June 2024

Keywords:
Type 1 diabetes
Glucagon
Identification
PK/PD models

ABSTRACT

The glucagon effect is understudied in type 1 diabetes (T1D) simulators, without a clear consensus on the pharmacodynamics of glucagon over glucose. Glucagon receptors dynamics could present a significant contribution to T1D simulators, making them more physiologically accurate without an excessive increase in complexity. This work analyzes the receptors model contributions to glucose dynamics using a model proposed in previous work. Then, the model is assessed from two different perspectives: (1) A clinical dataset of the influence of diet (high or low carbohydrate content) on two consecutive glucagon doses (100 and 500 μg) is used to identify the model parameters and (2) three other glucagon action models from the literature are also identified to serve as comparators. Different identification methods are used to adapt to the distinctive features of the dataset. The root mean square error (RMSE) and the Akaike Information Criterion (AIC) were the discerning metrics used to compare the models fittings. Results show that the receptors model offers the lowest RMSE and AIC in contrast to the comparators. This model will hence be helpful in the development of accurate T1D simulators.

© 2024 The Author(s). Published by Elsevier Ltd. This is an open access article under the CC BY-NC-ND license (http://creativecommons.org/licenses/by-nc-nd/4.0/).

1. Introduction

Mathematical models of biological processes facilitate experimentation when the real processes are unavailable, or the experiments are too complex or expensive (Balsa-Canto et al., 2010). In the context of human clinical experiments, mathematical models are usually employed to reproduce the effect of a particular substance or drug on the body. The models approximating these effects include the substance's pharmacokinetics (PK) and pharmacodynamics (PD). PK describes how the substance behaves from the administration point (e.g., oral ingestion, subcutaneous or intravenous administration) until its appearance in plasma, whereas PD represents its effect over a certain magnitude (e.g. effect on blood glucose levels) (Rimmington, 2020).

Normal blood glucose regulation relies on the coordinated secretion of several pancreatic hormones that keep glucose levels within a tight range. The main actors in glucose homeostasis are pancreatic hormones insulin and glucagon. Insulin, produced by β-cells, lowers blood glucose levels, and glucagon, produced in the α-cells, raises glucose levels (Woods et al., 2006). Glucose regulation can be affected by metabolic disorders, such as Type 1 Diabetes (T1D), characterized by the autoimmune destruction of β-cells. The consequent deficiency in endogenous insulin production makes patients dependent on the external administration of insulin. Additionally, sometimes other drugs are used to aid in the therapy management, such as glucagon, pramlintide, GLP-1 receptor agonists, or SGTL inhibitors (Avgerinos et al., 2021).

In order to ease insulin administration management, Automatic Insulin Delivery (AID) systems (also known as Artificial Pancreas, AP) were developed. These systems consist of a glucose sensor, an insulin pump, and a control algorithm that regulates insulin administration based on the sensor information (Lakshman et al., 2023). Multi-hormonal systems incorporate additional control actions, such as glucagon (Blauw et al., 2021).

Mathematical models are often used in diabetes-related research to test and validate control algorithms *in silico* prior to carrying out clinical trials (Ajmera et al., 2013). Simulators and models in the literature focused on T1D typically describe glucose changes as a response to insulin administration (Bergman, 2005).

* Corresponding author at: Instituto Universitario de Automática e Informática Industrial, Universitat Politècnica de València, C/Camí de Vera, s/n, València, 46022, Spain.
E-mail address: jbondia@isa.upv.es (J. Bondia).

https://doi.org/10.1016/j.ifacsc.2024.100272
2468-6018/© 2024 The Author(s). Published by Elsevier Ltd. This is an open access article under the CC BY-NC-ND license (http://creativecommons.org/licenses/by-nc-nd/4.0/).

Also, they may include the description of meal ingestion (Wilinska et al., 2010) or the PK/PD of other substances such as glucagon (Visentin et al., 2018) or pramlintide (Furió-Novejarque et al., 2024; Ramkissoon et al., 2014).

The glucagon effect is usually expressed as a contribution to endogenous glucose production (EGP) from the liver, being independent of the insulin effect (Dalla Man et al., 2014; Herrero et al., 2013; Kelly et al., 2019; Resalat et al., 2019). On the other hand, other EGP definitions consider a potential interference between insulin and glucagon (Emami et al., 2017; Smaoui et al., 2020; Wendt et al., 2017). However, the glucagon effect involves diverse mechanisms that are difficult to replicate. The study by El Youssef et al. (2014) observed that the glucagon effect was blunted in hyperinsulinemia conditions (a phenomenon approximated in the models by Wendt et al. (2017) and Emami et al. (2017)). Another concern surrounding glucagon is the potential loss of effectiveness in case of glycogen reserves depletion and whether repeated glucagon doses would contribute to their depletion (Blauw et al., 2016; Castle et al., 2015). Glycogen store levels are considered in the model by Benam et al. (2023), but it has only been validated with non-diabetic swine data. Additionally, the model presented by Hinshaw et al. (2015) accounted for the *evanescence* effect of glucagon (i.e., a decrease in the hormone effect over time). Some of these phenomena are still understudied. However, developing control algorithms for AP systems requires accurate simulators of the hormone effects.

As a conclusion, most models in the literature describe glucagon contribution to EGP as a magnitude proportional to the glucagon concentration (Dalla Man et al., 2014; Herrero et al., 2013; Kelly et al., 2019), which might be insufficient to properly describe glucagon behavior accurately. On the other hand, more complex models opt for functional approaches, sometimes adding states that do not have a physiological translation. For instance, the EGP models in Emami et al. (2017) and Resalat et al. (2019) consider an extra compartment that depends on the glucagon concentration's rate of change.

Aiming at providing a more physiological interpretation of the EGP process, the authors proposed in a previous work an EGP model based on glucagon receptors, which are primary mediators of the glucagon effect on EGP (Furió-Novejarque, Sanz et al., 2023). The model was validated against a dataset of clinical data where single doses of glucagon (100, 200, and 300 μg) were administered in mild-hypoglycemia conditions (Ranjan et al., 2016).

This work presents an extensive structural evaluation of the EGP model using a different clinical data set, extending the work presented in the IFAC WC (Furió-Novejarque, Sala-Mira et al., 2023). The proposal's performance is compared against three other EGP models from the literature based on their ability to fit the dynamics observed in the data. The dataset used in this work is particularly challenging since the trial evaluated the influence the carbohydrate content in the patients' diet had on glucagon effectiveness (i.e., the behavior of glucagon in both arms of the trial is different). This data will allow further testing of the capabilities of the proposed model.

The rest of the paper is divided as follows: Section 2 describes the Materials and Methods, presenting the models simulated in this work, the clinical dataset, the identification procedures, the PK identification methods, and the PD identification methods. Section 3 presents the results, including details on the parameter values, the models' execution, and the overall errors measured with each of them. Section 4 lays out a discussion of the presented results, and Section 5 summarizes the conclusions of the work.

2. Materials and methods

The proposed EGP is evaluated by comparing the root mean squared error (RMSE) and the value of the Akaike Information Criterion (AIC) obtained with the proposal against three other EGP definitions from the literature. The parameters of each EGP model are identified to fit a set of clinical data.

This section describes the model and the EGP comparators for the evaluation (Section 2.1). Next, the clinical dataset used to identify the models is described (Section 2.2), and Section 2.3 presents the identification materials used in the subsequent sections. Sections 2.4 and 2.5 describe the identification methods used for PK and PD, respectively.

2.1. EGP proposal and comparators

In order to adequately describe glucose dynamics, a complete PK/PD model is needed. Our analysis focuses on the definition of EGP, which is one of the contributors to the glucose regulation system.

The work in Furió-Novejarque, Sanz et al. (2023) proposed an EGP model based on glucagon receptor dynamics, following the work in Masroor et al. (2019). Plasma glucagon becomes effective when it binds to its receptors in the liver (Böhm et al., 1997), which triggers a chain of protein reactions that promote glycogenolysis (breakdown of glycogen to be translated into glucose) and gluconeogenesis (obtaining glucose from other sources such as lactate) (Müller et al., 2017). Glucagon receptors undergo a distinctive lifecycle, where the most representative states are *available*, *bounded*, and *internalized* (Koenig, 2004). The work by Masroor et al. (2019) simplified this three-state system into two differential equations, assuming the total number of receptors remains constant:

$$\dot{r}_c(t) = k_{on} \cdot V_h \cdot C(t) \cdot r(t) - k_{off} \cdot r_c(t) - k_{in} \cdot r_c(t) \tag{1}$$

$$\dot{r}(t) = -k_{on} \cdot V_h \cdot C(t) \cdot r(t) + k_{off} \cdot r_c(t) + k_{rec}(1 - r(t) - r_c(t)) \tag{2}$$

The state $r_c(t)$ represents the relative amount of active receptors, and $r(t)$ represents the available (unbound) receptors. The transfer rates k_{on}, k_{off}, k_{rec}, and k_{in} represent the transition of receptors from one state to another (available to active, active to available, internalized to available, and active to internalized.) The work in Furió-Novejarque, Sanz et al. (2023) modified the original proposal for the effect of glucagon on the hepatic glucose production proposed in Masroor et al. (2019), as well as the final expression of EGP, resulting in:

$$EGP(t) = \frac{V_r \cdot r_c(t)}{K_r + r_c(t)} + EGP_0(1 - S_I \cdot x_3(t)) \tag{3}$$

This definition considers glucagon dependent on the amount of active receptors through a Michaelis–Menten expression and includes a term to account for insulin effect ($x_3(t)$) on hepatic glucose production. Eqs. (1)–(3) were then integrated into a glucoregulatory model , which served as a baseline model. The model proposed in Wendt et al. (2017), based on the Hovorka model (Wilinska et al., 2010), was selected since it included descriptions of both insulin and glucagon PK. Table 1 includes the equations of the baseline model in *Baseline model* row. The following rows in the table present the equations of the proposed EGP as well as the definitions of the EGP models selected as comparators.

The criterion used to include EGP definitions as comparators was based on: (1) models that included glucagon dynamics, and (2) models whose underlying dynamics were based on Hovorka's PK/PD model. This criterion aimed to select models whose underlying structure was similar to the baseline model used in this

Table 1
Model equations for the complete system. The upper row describes the baseline model, which includes a PD subsystem and insulin and glucagon PK subsystems. This structure remains the same in every validation regardless of the EGP definition. The following rows describe the proposed EGP based on glucagon receptors, and the three EGP definitions selected as comparators, labeled EGP 1 (Wendt et al., 2017), EGP 2 (Emami et al., 2017), and EGP 3 (Jacobs et al., 2015). The function $\mathcal{H}$ in EGP 2 represents the Heaviside function, used to keep the expression positive. A detailed description of the state variables and parameters is included in the Appendix (Tables A.7 and A.8).

Structure	Equations
Baseline PK/PD model	Insulin PK: $\dot{S}_1(t) = u_I(t) - \frac{S_1(t)}{t_{max}}, \quad S_1(0) = 0$ $\dot{S}_2(t) = \frac{S_1(t)}{t_{max}} - \frac{S_2(t)}{t_{max}}, \quad S_2(0) = 0$ $I(t) = \frac{1}{t_{max}} \frac{S_2(t)}{W \cdot Cl_{F,I}} \cdot 10^6 + I_b$ Glucagon PK: $\dot{Z}_1(t) = u_C(t) - k_1 \cdot Z_1(t), Z_1(0) = 0$ $\dot{Z}_2(t) = k_1 \cdot Z_1(t) - k_2 \cdot Z_2(t), Z_2(0) = 0$ $C(t) = \frac{k_2 \cdot Z_2(t)}{W \cdot Cl_{F,C}} + C_b$ PD: $\dot{x}_1(t) = -k_{a1}[x_1(t) - I(t)], \quad x_1(0) = I_b$ $\dot{x}_2(t) = -k_{a2}[x_2(t) - I(t)], \quad x_2(0) = I_b$ $\dot{x}_3(t) = -k_{a3}[x_3(t) - I(t)], \quad x_3(0) = I_b$ $\dot{Q}_1(t) = -F_{01}^c(t) - F_R(t) - S_T \cdot x_1(t) \cdot Q_1(t) + k_{12} \cdot Q_2(t) + EGP(t)$ $\dot{Q}_2(t) = S_T \cdot x_1(t) \cdot Q_1(t) - [k_{12} + S_D \cdot x_2(t)] Q_2(t)$ $Q_1(0) = G_0, \quad Q_2(0) = Q_2(t)\|_{Q_1(t)=Q_1(0), x_2(t)=x_2(0)}$ $G(t) = \frac{Q_1(t)}{V}$ $F_{01}^c(t) = \begin{cases} F_{01} & \text{if } G(t) \geq 4.5 \text{ mmol/L} \\ F_{01} \cdot G(t)/4.5 & \text{otherwise} \end{cases}$ $F_R(t) = \begin{cases} 0.003(G(t) - 9)V_G & \text{if } G(t) \geq 9 \text{ mmol/L} \\ 0 & \text{otherwise} \end{cases}$
Proposed EGP	$EGP(t) = \frac{V_r \cdot r_c(t)}{K_r + r_c(t)} + EGP_0(1 - S_I \cdot x_3(t))$ $\dot{r}_c(t) = k_{on} \cdot V_h \cdot C(t) \cdot r(t) - k_{off} \cdot r_c(t) - k_{in} \cdot r_c(t)$ $\dot{r}(t) = -k_{on} \cdot V_h \cdot C(t) \cdot r(t) + k_{off} \cdot r_c(t) + k_{rec}(1 - r(t) - r_c(t))$ $r_c(0) = r_c(t)\|_{C(t)=C_b}, \quad r(0) = r(t)\|_{C(t)=C_b}$
EGP 1	$EGP(t) = G_{GG}(t) + G_{GNG}$ $G_{GG}(t) = \frac{1 - S_e \cdot x_3(t)}{1 - S_E \cdot I_b} \left((E_{max} - G_{GNG}) \cdot \frac{C(t)}{C_{E50} + C(t)} \right)$
EGP 2	$EGP(t) = \mathcal{H}(1 - S \cdot x_3(t)) \cdot \mathcal{H}(EGP_G(t) + T \cdot C(t)) + G_{ng}$ $\dot{EGP}_G(t) = -k_{Gd} \cdot EGP_G(t) - k_{Gd} \cdot T_{Gd} \cdot \dot{C}(t), \quad EGP_G(0) = 0$
EGP 3	$EGP(t) = EGP_0\left(1 - S_f \cdot x_3(t) + Y(t) + k_{g3} \cdot \dot{Y}(t)\right)$ $\dot{Y}(t) = k_c \cdot C(t) - k_d \cdot Y(t), \quad Y(0) = Y(t)\|_{C(t)=C_b}$

work. Thus, the chances of negatively affecting the EGP model performance due to the change in the glucoregulatory model would be minimized.

The selected EGP expressions to serve as comparators have been labeled as EGP 1, EGP 2, and EGP 3. The first one was presented in Wendt et al. (2017) alongside the base model used in this work (see Table 1, EGP 1 row). It relates glucagon and insulin concentrations in such a way that insulin limits the glucagon effect in an effort to replicate the phenomena observed in El Youssef et al. (2014). EGP 2 was proposed in Emami et al. (2017) as the result of fitting nine model structure candidates to the data in El Youssef et al. (2014). The models in Emami et al. (2017) range from two-parameter expressions to systems with five parameters and additional differential equations. Model-fitting results in that work showed how the simpler models were not able to explain the glucagon effects observed in the data (Emami et al., 2017). Hence, the final selection corresponds to their proposal number 8 (Table 1, EGP 2 row). The definition of EGP 3 was first presented in Jacobs et al. (2015), where the baseline model was also based on the Hovorka model. Their proposal incorporates an approximation of the glucagon effect using a remote compartment ($Y(t)$) and is also dependent on the glucagon rate of change, $\dot{Y}(t)$ (Table 1, EGP 3 row).

For a complete description of the model parameters, as well as the EGP comparators, see Tables A.7 and A.8 in the Appendix.

2.2. Identification data

Models were fit with the datasets of the clinical trial by Ranjan et al. (2017), provided by the Steno Diabetes Center in Copenhagen. This clinical trial consisted of two arms that assessed the impact of the diet's carbohydrate content on glucagon effectiveness on glucose in ten people with T1D.

Each arm consisted of an outpatient week and a clinical visit. During the outpatient week, patients were required to follow a diet with different carbohydrate content depending on the study arm: a high carbohydrate content diet (HCD) of 250 g/day and a low carbohydrate content diet (LCD) of 50 g/day. During the in-clinic visit, patients were administered an insulin bolus on arrival to lower their glucose values. When plasma glucose levels dropped below 70 mg/dL, they were administered a 100-μg glucagon bolus, followed by a dose of 500 μg two hours later. Patients were monitored for two more hours after the second glucagon dose. Fig. 1 summarizes the available data, including plasma glucose, insulin, and glucagon. The results are grouped by visit: after the LCD (labeled Visit L) or the HCD (labeled Visit H).

Ranjan et al. (2017) reported that glucose response to glucagon after LCD was lower than after HCD, suggesting that LCD reduces hepatic glycogen stores, a primary mediator of glucagon effect during glycogenolysis (Shrayyef & Gerich, 2010). Glycogen deficiency is one of the concerns regarding the use of glucagon in closed-loop systems since some studies suggest that a repeated administration of glucagon may deplete glycogen reserves, causing a reduction in glucagon effectiveness (Bélanger et al., 2000; Blauw et al., 2016). On the other hand, another study observed no depletion of glycogen reserves after repeated glucagon administration (Castle et al., 2015).

Table 2 summarizes the differences in the maximum glucose increase achieved with both glucagon doses in the two experimental settings. The most affected dose due to the diet difference is the 100 μg dose, which has its average value reduced to half in the LCD arm (ΔG_{100}), compared to the HCD. This reduction is

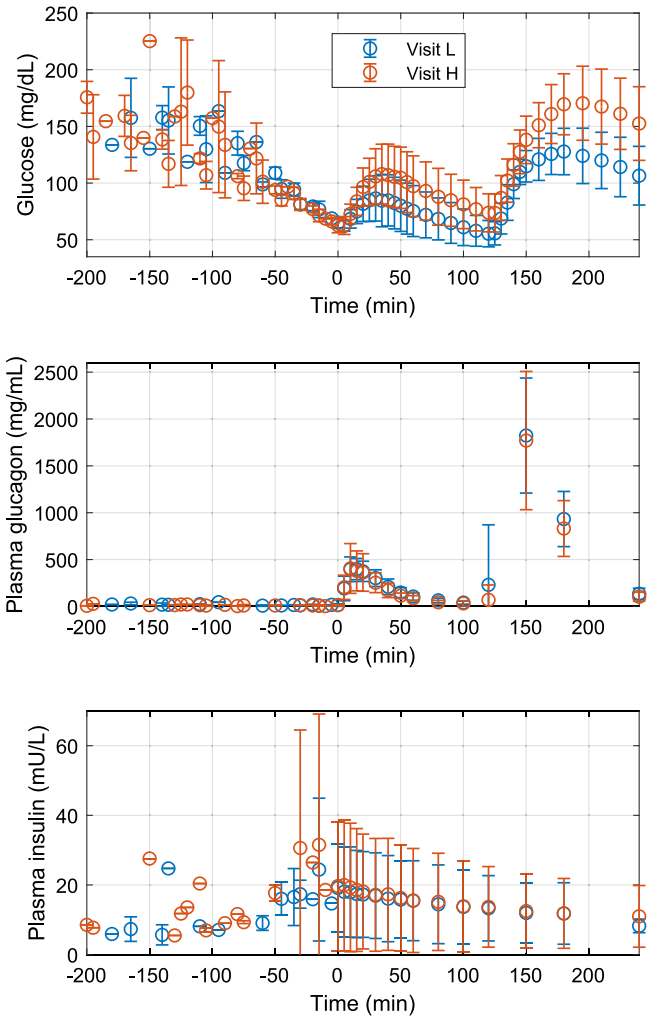

Fig. 1. Mean values and standard deviations of the data from the clinical trial in Ranjan et al. (2017). Available data included plasma glucose (upper graph), plasma glucagon (middle graph), and plasma insulin (bottom graph). Data in blue represent Visit L (low carbohydrate content diet arm), and data in orange represent Visit H (high carbohydrate content diet arm). An insulin bolus was administered on arrival at the clinic, and when reaching 70 mg/dL, the first glucagon dose (100 μg) was administered (time $t = 0$). The second dose (500 μg) was given 2 h later. (For interpretation of the references to color in this figure legend, the reader is referred to the web version of this article.)

Table 2
Mean ± standard deviation of glucose values and increments depending on the dose, expressed in mg/dL. G_{100} represents the glucose value at the time of the 100 μg administration. ΔG_{100} is the maximum increment observed after the 100 μg dose. G_{500} and ΔG_{500} represent the same concepts for the 500 μg counterpart.

Trial arm	G_{100}	ΔG_{100}
LCD	65.02 ± 4.47	22.87 ± 19.90
HCD	62.64 ± 6.49	47.28 ± 23.25
	G_{500}	ΔG_{500}
LCD	55.36 ± 11.62	73.23 ± 11.15
HCD	73.76 ± 16.80	100.66 ± 25.63

not so abrupt in the 500 μg dose, where there is an approximate reduction of 27% (ΔG_{500}). Also note that, although several trials have demonstrated that small glucagon doses (i.e., 100 μg) are sufficient to help recover from hypoglycemia (Haymond et al., 2016; Laugesen et al., 2023; Ranjan et al., 2016), said dose was ineffective in the LCD setting since 2 h later to the administration of the dose (glucose value at G_{500}, Table 2) glucose values are below the hypoglycemia range (average of 55.36 mg/dL).

Nonetheless, the results from this clinical trial provide a very interesting dataset for evaluating different glucagon effect descriptions. The validation in Furió-Novejarque, Sanz et al. (2023) used a dataset that included the administration of glucagon doses of 100, 200, and 300 μg. This new dataset provides a broader range of doses (100 μg and 500 μg) under different settings (LCD and HCD). Testing consecutive administration is important since internalization of glucagon receptors could affect the dynamics of newly administered doses of glucagon.

2.3. Identification materials

In order to identify the parameters of each EGP model, an optimization process assessed the difference between the simulation output and the data points. This difference was evaluated using the RMSE, which is defined as follows:

$$\text{RMSE}^{v}_{P,m} = \sqrt{\frac{1}{n_v}\sum_{i=1}^{n_v}(e^{v}_{P,m})^2} \tag{4}$$

$$\text{where} \quad e^{v}_{P,m} = \hat{y}^{v}_{i,P,m} - y^{v}_{i,P,m}$$

In the datasets available, a given patient would participate in both arms of the clinical trial. Hence, multiple visits to the clinic ensued. The subscript P in Eq. (4) denotes a specific patient, v denotes a visit (L or H), and m refers to the model used. The number of data points in the specific experiment is indicated by n_v, the model output is $\hat{y}_{i,P}$, and $y^{v}_{i,P}$ represents the set of data points.

The optimization aimed to find the parameter combination that minimized the index J_P per patient. The definition of the index was dependent on the evaluated method, but in every case, it was a function of the RMSE obtained in the simulation.

$$J_P = f(RMSE^{v}_{P,m}) \tag{5}$$

The optimization was carried out in Matlab using a local optimization solver (`fmincon`). In order to avoid local minima, the optimizations were run ten times and the one with the lowest index was selected as the solution. The initial points were different each time the optimizer was executed, being drawn from a Latin hypercube sampling (McKay et al., 2000). Models were simulated with Matlab's `ode45` function. Initial conditions for the simulations are included in Table 1. These were derived from steady state relations (derivatives set to 0), considering that the glucose, plasma glucagon, and plasma insulin measured at the trial start, i.e., $G(0) = G_0$, $C(0) = C_b$, and $I(0) = I_b$ correspond to equilibrium conditions.

The latter assessment of the identification results was based on the comparison of the RMSE and AIC obtained with the proposal, against the three EGP comparators. AIC is a common selection criteria in the context of biological models (Faggionato et al., 2023; van Sloun et al., 2023), defined as:

$$AIC = N \cdot \ln\left(\frac{SSR}{N}\right) + 2 \cdot K, \tag{6}$$

where N represents the number of data samples, K is the number of parameters in the model, an SSR stands for "sum of squared residuals", defined in Eq. (7).

$$SSR = \sum(\hat{y}_i - y_i)^2 \tag{7}$$

2.4. PK identification

The parameters in the baseline model were unknown for this cohort. However, having plasma insulin and glucagon data, it was possible to perform separate identifications for the respective PK subsystems, measuring the error with respect to the insulin and plasma glucagon concentrations, respectively, and focusing afterward on glucose dynamics in the glucose data.

The insulin PK parameters (see Table 1) to be identified were:

$$\theta_{I-PK} = \left\{t_{max}, Cl_{F,I}\right\}$$

The value of basal insulin (I_b) was taken from the end values of plasma insulin data. On the other hand, parameters in the glucagon PK subsystem (Table 1) were:

$$\theta_{G-PK} = \left\{k_1, k_2, Cl_{F,C}\right\}$$

The parameter corresponding to the patient's weight (W) appeared in both subsystems. Since the individual value of W for each patient was not available, it was assumed constant, equal to the median weight of the patients participating in the trial (75.2 kg, see Table 3).

Regarding the identification of plasma insulin, the data was undersampled in the first part (before $t = 0$), corresponding with the initial insulin bolus administration. This makes the pharmacokinetics of insulin difficult to infer since only the "tail" of the bolus is captured (see Plasma insulin plot in Fig. 1).

A collection of identification strategies was carried out to find the most appropriate parameter values for PK. The final values of the parameters for each patient were selected from two of those identification sets based on an assessment of the error observed in the second part of the data (from $t = 0$ onward), where a higher amount of data points were registered.

On the other hand, the identification of glucagon PK presented a similar issue in the sampling corresponding to the second glucagon dose (t between 120 and 240 min). Moreover, individual analysis of the data and the preliminary identification results showed that (1) there were slight but noticeable differences in the glucagon plasma response from one visit to another (visit L versus visit H) and (2) the behavior of the plasma glucagon increase was nonlinear, meaning that fitting the first smaller dose did not provide an adequate fit in the second dose (based on the spare data points available), and vice-versa.

Hence, in order to achieve the most accurate description of the plasma glucagon signal, an individual adjustment of the glucagon PK identified values was performed so that for some patients, values for k_2 were different from one visit to the other, but also for each of the glucagon doses. The value of $Cl_{F,C}$ also had to be adjusted for the bigger dose from one visit to the other.

The parameter values identified for θ_{I-PK} and θ_{G-PK} remained the same for all the subsequent identifications.

2.5. PD identification

A set of parameters had to be identified for the baseline model, regardless of the EGP definition. A global sensitivity analysis was carried out in order to assess the practical identifiability of the system and help determine which parameters should be considered for the identification process. The analysis was carried out using Matlab toolbox AMIGO2 (Balsa-Canto et al., 2016). A constraint was introduced in the simulations to discard the experiment if glucose reached values under 32.5 mg/dL or above 450 mg/dL. This way, the software discarded the parameter combinations that resulted in non-physiological behaviors for the given inputs: 100 and 500 μg of glucagon.

The toolbox quantifies the influence of each parameter on the output by the mean squared sensitivity (MSQRT) proposed by Brun et al. (2001). The higher the value, the greater influence on the observed variable. To simplify the interpretation of the results, the relative MSQRT, obtained by dividing the MSQRT of the parameter by the sum of all MSQRTs, was also computed. The relative MSQRT can be used to classify the parameters in three sensitivity clusters (Garcia-Tirado et al., 2018): (1) *sensitive parameters* are the first parameters in order of MSQRT summing more than the 80% of the total MSQRT (i.e, the sum of the relative MSQRT is larger than 0.8); (2) *insensitive parameters* are the parameter subsets which accumulates less than the 1% of the total MSQRT; and (3) *mildly sensitive parameters* are remaining ones.

Table 3
Baseline model parameters set to constant values in the simulations.

Parameter	k_{a2}	k_{a3}	V	W
Units	(min^{-1})	(min^{-1})	(mL/kg)	(kg)
Value	$489 \cdot 10^{-4}$	$118 \cdot 10^{-4}$	160	75.2

Table 4
Glucagon receptors model parameters set to constant values in the simulations.

Parameter	k_{off}	k_{rec}	k_{in}	V_h
Units	(min^{-1})	(min^{-1})	(min^{-1})	(L)
Value	0.24	0.003	0.358	4.65

The analysis results for PD parameters of the baseline model are presented in Fig. 3. Based on the observations, parameters F_{01} and S_t are sensitive parameters, whereas k_{a2} and k_{a3} can be considered insensitive. Following Garcia-Tirado et al. (2018), the insensitive parameters k_{a2} and k_{a3} were discarded for being identified and were set to constant values, based on previous identifications of this system (Furió-Novejarque, Sala-Mira et al., 2023). Table 3 includes their values, as well as the value for glucose distribution volume, V, that was set following Wendt et al. (2017).

Due to the often observed variability in the patients' insulin sensitivity, one of the related parameters (S_T and S_D) was identified for each visit to the clinic (L or H). Based on the sensitivity analysis, S_T was selected. Hence, the list of parameters to be identified from the baseline model becomes:

$$\theta_{1P} = \left\{S_T^v, S_D, F_{01}, k_{12}, k_{a1}\right\}$$
$$P = 1, 2, \ldots, 10; \quad v = \text{L, H}$$

where v and P correspond to the visit and subject index the parameters have been individualized to.

Then, a set of parameters was identified for each EGP definition. Starting with the receptors proposal, the parameter vector included:

$$\theta_{2P} = \{EGP_0, S_I, k_{on}, K_r, V_r\}, \quad P = 1, 2, \ldots, 10$$

Among the transfer rates comprising the system (k_{off}, k_{rec}, k_{on}, k_{in}), only the activation rate of glucagon receptors, k_{on} was identified to avoid identifiability issues (Masroor et al., 2019). The remaining rates were set to constant values based on transfer rate values from the literature, as reported in Masroor et al. (2019). The value for k_{off} was taken from Ronald Kahn (1976), and the recycling constant for glucagon receptors, k_{rec}, is assumed to be equal to insulin receptors, taking the value reported in Sedaghat et al. (2002). Lastly, k_{in} was set based on the identification in Masroor et al. (2019), where the value of V_h was also taken. Table 4 includes the values set for each of the aforementioned parameters.

Regarding the EGP comparators, the EGP 1 model only required four parameters:

$$\theta_{3P} = \{G_{GNG}, S_E, E_{max}, C_{E50}\}, \quad P = 1, 2, \ldots, 10$$

On the other hand, EGP 2 and EGP 3 consisted of five parameters, similar to the EGP proposal.

$$\theta_{4P} = \left\{G_{ng}, S, T, K_{Gd}, T_{Gd}\right\}, \quad P = 1, 2, \ldots, 10$$

$$\theta_{5P} = \left\{EGP_0, S_f, k_{g3}, k_d, k_c\right\}, \quad P = 1, 2, \ldots, 10$$

The resulting parameter vector to be identified per patient contained a total of 25 parameters:

$$\Theta_P = \left\{\theta_{1P}^v, \theta_{2P}, \theta_{3P}, \theta_{4P}, \theta_{5P}\right\}$$

Having defined the set of parameters to identify, the combination of the baseline model plus each EGP model was used to simulate both visits. All the parameters for each EGP definition plus the baseline PD model were identified in the same optimization process, and the total optimization index was defined as a function of the RMSE obtained with each of them. However, a progressive refinement of the identification method was carried out, which led to three sets of results, one for each method. The following subsections describe said methods and the justification that led from one to another.

Of note, moving forward, the name of each EGP model will refer to the combination of that EGP definition plus the baseline model.

2.5.1. Method A

The optimization cost index J_P (5) was computed as the average of the sum of the total RMSE of each simulation (L and H) with each of the four models (m):

$$J_P = \frac{1}{n_m}\sum_{m=1}^{n_m}\sum_{v=1}^{n_v} RMSE_{P,m}^v \tag{8}$$

The parameters n_v and n_m represent the number of visits and the number of models, respectively. $RMSE_{P,m}^v$ (4) represents the total RMSE obtained in a simulation with a particular model (m) in a determinate visit v (L or H). The average of the sum of these two magnitudes, per each of the four models, constituted the optimization index J_P.

The results obtained with this method are labeled Method A in the Results section. One of the criteria to perform a fair comparison between the execution of each model was that they behaved the same (or as similarly as possible) during the first part of the data, prior to the first glucagon dose when only the effect of insulin was active. The focus of the analysis is to study how the model structures differ in the glucagon description. If part of that difference was already accounted for in the basal value of EGP, then it may yield a misleading interpretation. The results obtained in this stage showed that using the same parameters in the baseline model was insufficient to eliminate the errors between models in the first part of the data (before the first glucagon dose). See Fig. 4, upper row plots, for a sample of the results obtained for Patient 3 with this method.

2.5.2. Method B

A second approach to the identification was followed. The error in the first period was penalized more than the others to reduce the differences between models observed with Method A. With this, the error calculation, $e_{P,m}^v$ in Eq. (4), was redefined as:

$$e_{P,m}^v = \begin{cases} \omega \cdot (\hat{y}_{i,P,m}^v - y_{i,P,m}^v), & \text{if } t \le t_{100} \\ (\hat{y}_{i,P,m}^v - y_{i,P,m}^v) & \text{if } t > t_{100} \end{cases} \tag{9}$$

The value of ω was set to 10, and t_{100} refers to the time of the first glucagon dose. The results for this identification are labeled as Method B. J_P was obtained following the same formula as in Method A (see Eq. (8)). This helped to significantly improve the fit in the first part of the data and the main differences between the models were displaced to the periods where glucagon was administered.

2.5.3. Method C

The main characteristic of this dataset is the difference in glucose response to glucagon caused by the diet. Methods A and B aimed to fit every situation (LCD and HCD) with the same glucagon model. However, the results show that the RMSE values for the visit H were consistently higher than for the visit L. The difference in diets is not accounted for in any of the models, so one of the visits is favored to the detriment of the other in the identifications. The last optimization carried out in this work tries to describe this difference in diet, optimizing a variable gain in each of the EGP models per visit.

The parameters were selected based on the global parameter sensitivity analysis results of each EGP definition (see Fig. 3).

The selected parameters were V_r for the receptors model, E_{max} for the EGP 1 model, T for the EGP 2 model, and EGP_0 for the EGP 3 model. Notice that the parameter selected for EGP 2 is not the most sensitive (G_{ng}), but the second (T). Focusing on the equations of EGP 2 (Table 1), G_{ng} represents an offset in the EGP expression, whereas T is a factor that directly affects glucagon concentration, a feature shared by the other parameters selected to be individualized. Consequently, given that the values of relative MSQRT of both parameters were similar, T was selected as the variable gain. The identification results obtained with this modification are labeled as Method C.

3. Results

3.1. PK results

The average parameters obtained in the identification of insulin and glucagon PK are described in Table A.9. Results are expressed as mean ± standard deviation. The table shows the parameters identified from the plasma glucagon signal, with an individualized parameter of k_2 per visit (L and H) and per dose (100 and 500 μg). The values of $Cl_{F,C}$ were the same regardless of the visit for the smaller dose, but they had to be adjusted for the second dose ($Cl_{F,CL-500}$ and $Cl_{F,CH-500}$).

Fig. 2 shows the aggregated results obtained in the simulations of plasma insulin and plasma glucagon for the ten patients.

3.2. PD results

Table A.10 shows the average values obtained for the parameters of each EGP definition and the PD subsystem of the baseline model. The parameters in Method C fitted for each visit are marked with a label L or H to the right of the parameter. The reported values aggregate the results obtained with the ten patients in the cohort.

Fig. 4 details the execution results obtained for patient 3 for each of the employed identification methods. The top row plots show visit L and H responses obtained for Method A. The middle row plots show the results obtained for Method B. As exposed in the previous section, this method was designed to correct the differences between models, and indeed, there is a reduction of the output differences during the time before the first glucagon dose. The bottom row plots show the results obtained for Method C. An improvement of the fit can be observed for some models, especially for visit H.

The upper row in Fig. 5 shows the RMSE results separated per model and method. It presents the RMSE progression from one method to another and the overall performance of each model structure. There is an overall RMSE increase after introducing the restriction to fit the first period of the data in Method B. Nevertheless, the RMSE obtained with the receptors proposal is consistently the lowest. The lower row in Fig. 5 presents the AIC results also separated per model and identification method.

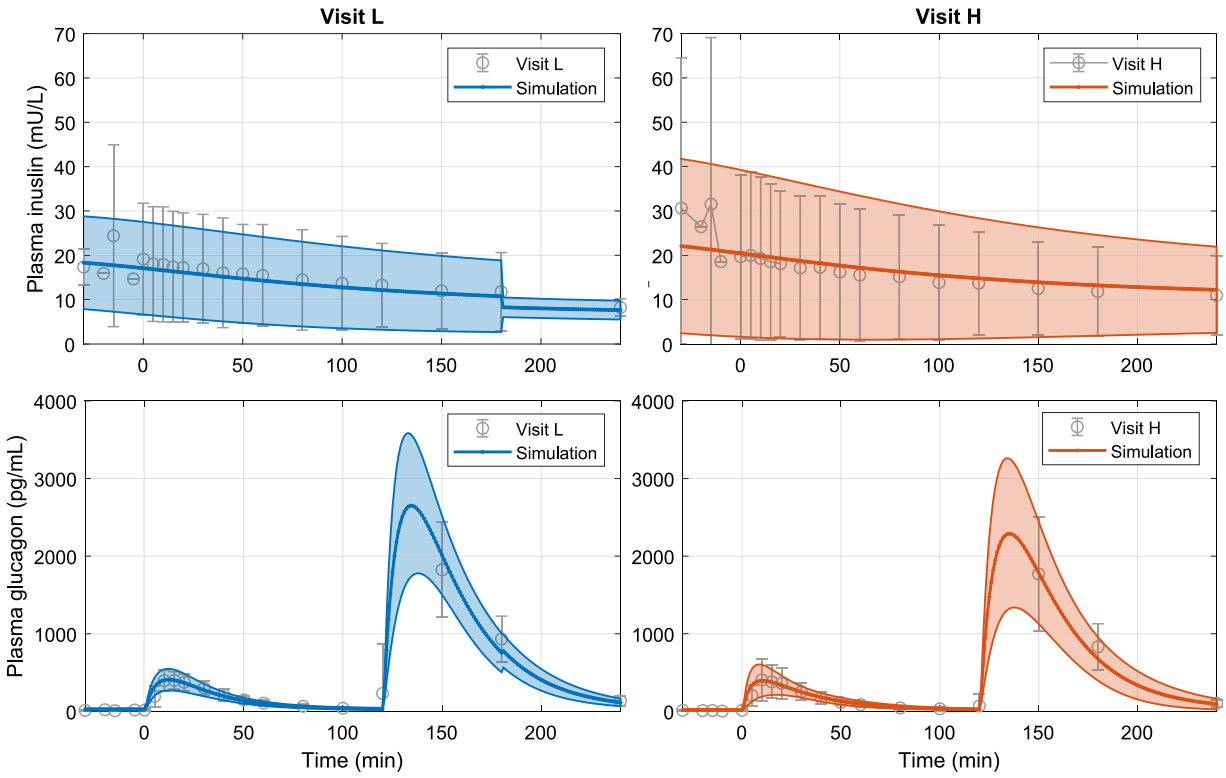

Fig. 2. Plasma insulin (top row) and glucagon (bottom row) simulation results. Gray error bars correspond to the mean and standard deviation of the data, and continuous/colored lines encase the mean and standard deviation of the simulation results. Graphs show the response from $t = 0$ min to 240 min, which is the main period of interest of the study. (For interpretation of the references to color in this figure legend, the reader is referred to the web version of this article.)

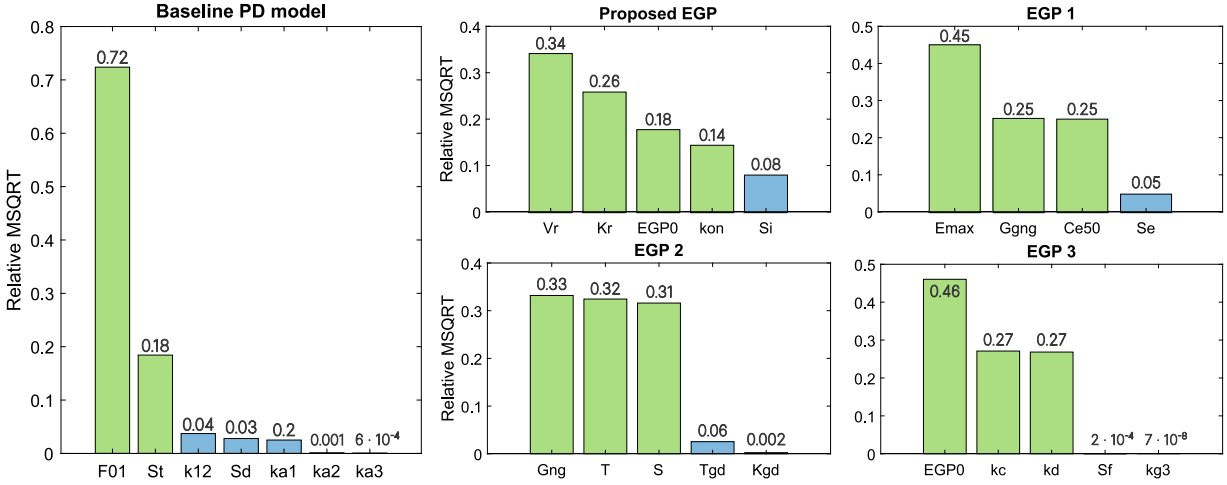

Fig. 3. Sensitivity analysis results for the baseline PD model parameters and each of the parameter sets in the EGP definitions (Proposed EGP, EGP 1, EGP 2, and EGP 3). The magnitude relative MSQRT represents the importance the parameter has on the system output. Color bars represent sensitivity clusters, based on Garcia-Tirado et al. (2018): green bars represent *sensitive parameters*, and blue bars, *mildly sensitive* parameters. The analysis was conducted using AMIGO2 Matlab toolbox (Balsa-Canto et al., 2016). (For interpretation of the references to color in this figure legend, the reader is referred to the web version of this article.)

This metric evaluates the ability of the model to fit the data and includes a penalization on the number of parameters in the model. Similar to the results obtained for the RMSE, the proposed EGP achieves the lowest average AIC.

A statistical analysis was carried out in R (version 4.1.3) to analyze the differences between the results obtained with the receptors model and the comparators. Once ensured data distributions followed a normal distribution through the Kolmogorov–Smirnov test, a paired t-test was calculated between the receptors model and each EGP comparator to determine if any statistically significant difference existed at level 0.05. Table 5 presents the results of these analyses, separated by method and grouped by visits and the overall RMSE of the two visits. Of note, the RMSE difference in the overall results of each method is statistically significant in every case according to the p-value results. Besides the significance test, Cohen's d size effect measurement was also included to complement these results. This metric quantifies the size of the difference between two sets. The conventional

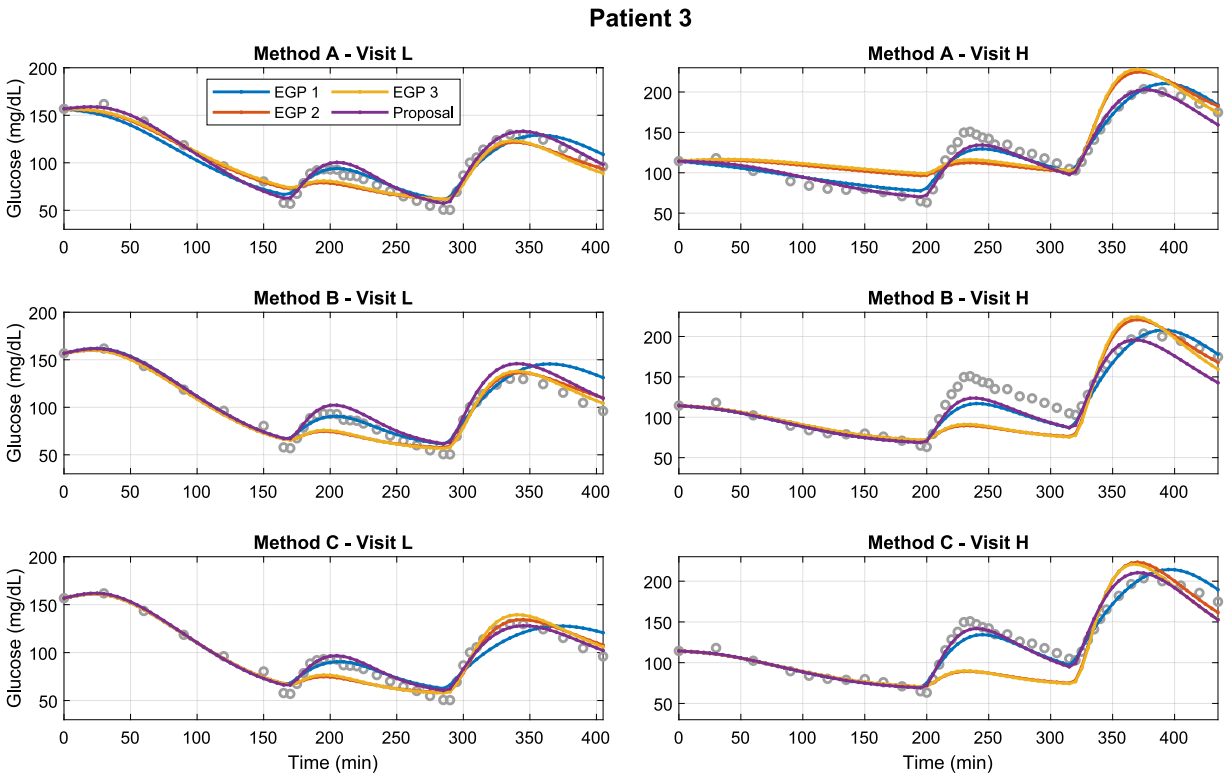

Fig. 4. Patient 3 results for identification Method A (top row), Method B (middle row), and Method C (bottom row). Gray circles represent the glucose data points. Continuous lines represent the simulations of the baseline model plus the EGP 1 (blue line), EGP 2 (orange line), the EGP 3 (yellow line), and the proposed EGP (purple line); for visit L (left column), and visit H (right column). (For interpretation of the references to color in this figure legend, the reader is referred to the web version of this article.)

Table 5
Comparison of RMSE (mg/dL) for each model and identification method, considering the average RMSE for the ten patients in the dataset in visits L and H, separated by visits. Values are expressed as mean ± standard deviation. The t-statistic and the p-value correspond to independent paired t-tests comparing every model against the proposed model. Cohen's d measures the effect size, with values over 0.8 considered a large difference (McGough & Faraone, 2009). These conditions have been highlighted with green-tinted cells.

Identification method	Visit	Model	Comparators RMSE	Proposal RMSE	t	p	Cohen's d
A	L	EGP 1	7.9 ± 2.3	7.0 ± 1.8	2.20	0.056	0.70
		EGP 2	9.2 ± 3.6		1.87	0.094	0.59
		EGP 3	9.4 ± 4.3		1.65	0.133	0.52
	H	EGP 1	10.2 ± 2.0	9.3 ± 2.0	2.49	0.035*	0.79
		EGP 2	13.7 ± 4.2		3.13	0.012*	0.99
		EGP 3	14.1 ± 4.2		3.62	0.006*	1.14
	Overall	EGP 1	9.0 ± 1.4	8.1 ± 1.1	2.88	0.018*	0.91
		EGP 2	11.4 ± 3.1		2.87	0.019*	0.91
		EGP 3	11.7 ± 3.5		2.84	0.019*	0.90
B	L	EGP 1	14.3 ± 7.6	13.1 ± 7.9	0.90	0.392	0.28
		EGP 2	15.9 ± 9.0		1.07	0.313	0.34
		EGP 3	15.7 ± 9.2		0.92	0.380	0.29
	H	EGP 1	18.7 ± 5.8	15.5 ± 7.8	2.01	0.075	0.64
		EGP 2	22.6 ± 6.5		2.43	0.038*	0.77
		EGP 3	23.8 ± 6.1		3.47	0.007*	1.10
	Overall	EGP 1	16.5 ± 6.0	14.3 ± 7.3	2.64	0.027*	0.83
		EGP 2	19.3 ± 6.4		2.22	0.053	0.70
		EGP 3	19.7 ± 6.6		2.62	0.028*	0.83
C	L	EGP 1	12.3 ± 4.3	10.1 ± 4.5	2.07	0.069	0.65
		EGP 2	13.1 ± 7.5		1.11	0.295	0.35
		EGP 3	16.3 ± 9.6		2.02	0.074	0.64
	H	EGP 1	13.1 ± 3.5	11.4 ± 5.0	0.86	0.412	0.27
		EGP 2	20.5 ± 6.5		3.36	0.008*	1.06
		EGP 3	23.7 ± 5.5		4.72	0.001*	1.49
	Overall	EGP 1	12.7 ± 2.0	10.8 ± 4.2	1.66	0.132	0.52
		EGP 2	16.8 ± 5.5		2.69	0.025*	0.85
		EGP 3	20.0 ± 6.3		3.89	0.004*	1.23

* Indicates a statistically significant difference at 0.05.

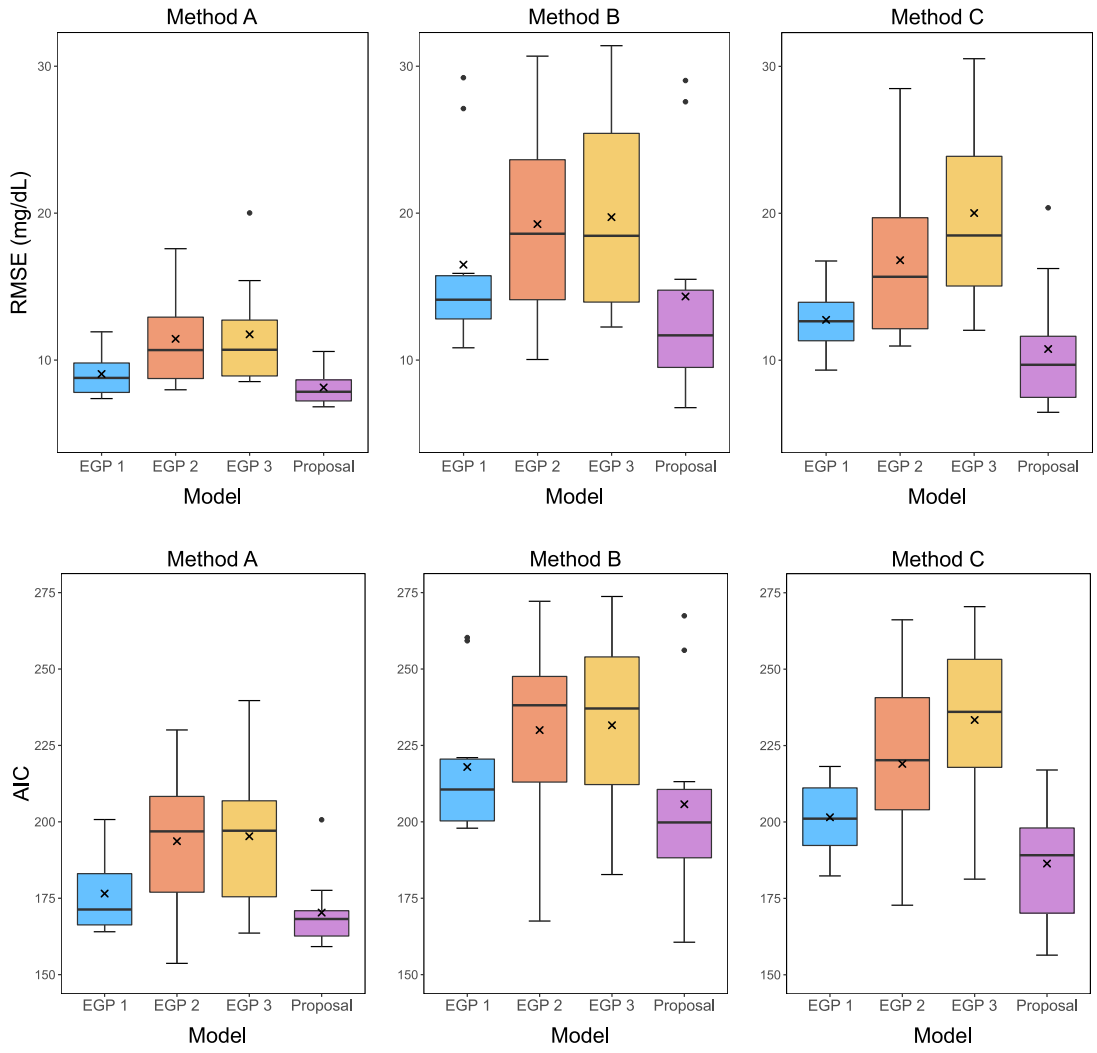

Fig. 5. Boxplots of overall RMSE (mg/dL) (upper row) and AIC (lower row) obtained for each identification method, separated per model. The displayed results aggregate the outcomes obtained with the ten patients in the dataset in both visits (L and H).

Table 6
Comparison of overall AIC for each model and identification method, considering the average AIC across visits (L and H) for the ten patients in the dataset. Values are expressed as mean ± standard deviation. The t-statistic and the p-value correspond to independent paired t-tests comparing every model against the proposed model. Cohen's d measures the effect size, with values over 0.8 considered a large difference (McGough & Faraone, 2009). These conditions have been highlighted with green-tinted cells.

Identification method	Model	Comparators AIC	Proposal AIC	t	p	Cohen's d
A	EGP 1	176.5 ± 13.1	170.3 ± 11.3	2.48	0.035*	0.78
	EGP 2	193.7 ± 24.0		3.02	0.015*	0.95
	EGP 3	195.3 ± 23.7		3.17	0.011*	1.00
B	EGP 1	217.9 ± 22.5	205.7 ± 31.2	2.28	0.049*	0.72
	EGP 2	230.0 ± 30.2		2.38	0.041*	0.75
	EGP 3	231.6 ± 28.6		2.81	0.020*	0.89
C	EGP 1	201.5 ± 11.7	186.4 ± 20.9	1.92	0.087	0.61
	EGP 2	219.0 ± 28.3		3.05	0.014*	0.96
	EGP 3	233.4 ± 26.5		4.58	0.001*	1.45

* Indicates a statistically significant difference at 0.05.

interpretation of Cohen's d values considers a 0.2 value represents a small difference, 0.5 is a medium effect, and 0.8 or a higher value indicates a large difference (McGough & Faraone, 2009). The significance of the difference between the results obtained with the receptors proposal and the EGP comparators is further reinforced by Cohen's d values greater than 0.8 in the overall results obtained with the three methods, as highlighted with green-tinted cells in Table 5. The same analysis was conducted for the average AIC values (Table 6).

The analysis is extended in Fig. 6, which differentiates the results per visit but also considers the three time periods given by the data:

- Period 1: from the start of the trial to the administration of the first glucagon dose (100 μg), where only the insulin

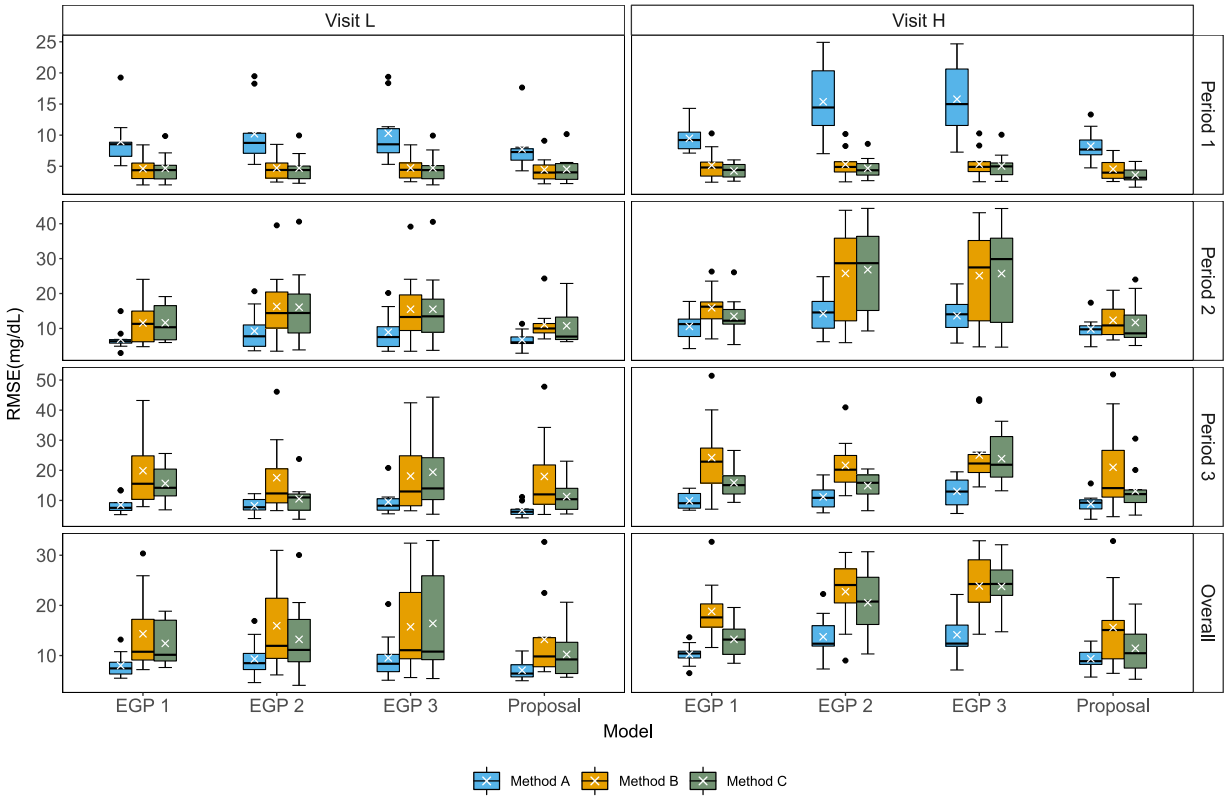

Fig. 6. General RMSE (mg/dL) comparison between Method A (blue boxes), Method B (orange boxes), and Method C (green boxes). Rows represent the considered period times (Period 1 to 3, or overall experiment time). The "Overall" row considers the total time of the experiment. Columns represent the visits (L or H). (For interpretation of the references to color in this figure legend, the reader is referred to the web version of this article.)

effect is significant, and EGP contribution is limited to its basal value.

- Period 2: from the administration of the first glucagon dose to the second (500 μg).
- Period 3: from the second glucagon dose to the end of the trial.

Some general conclusions can be drawn from Fig. 6: (a) The mean RMSE values are lower in the visit L identification than in the visit H; (b) In visit L, the error values for the smaller dose (Period 2) are similar to those for the second dose (Period 3), but in visit H, the difference between errors in periods 2 and 3 is larger; (c) The receptors model provides the lowest mean values in each studied situation, regardless of the identification method used.

4. Discussion

The results presented in Section 3 support the conclusions in Furió-Novejarque, Sanz et al. (2023) that an EGP model based on glucagon receptors dynamics may provide a more accurate description of the glucose response to glucagon. Compared to Furió-Novejarque, Sanz et al. (2023), the receptors model was evaluated with a larger glucagon maximum dose (500 μg vs. 300 μg), making the potential improvement of the receptors model over the remaining comparators more noticeable. In this evaluation, the RMSE and AIC results favor the proposal results, regardless of the identification method used.

Method A. Fig. 5 shows that, in Method A, the receptors model achieved a lower overall error compared to the rest of the EGP models. Note, however, that differences exists across periods (Fig. 6): while on periods 2 and 3, all models have close average RMSE values (Fig. 6, Period 2 and 3 rows, blue boxes), the most considerable difference was observed on Period 1, whose absolute error values are higher than in the other periods. These results show that, in general, the optimization tried to reduce possible errors in these periods by sacrificing the fit in the first part, which justifies weighting the first part of the data as proposed in Methods B and C.

Method B. Overall, the RMSE has augmented regarding the results with Method A, but the receptors model still yields a more accurate fit. Penalizing the error in Period 1 results in a remarkable reduction of the RMSE in this period compared to Method A but to the detriment of Periods 2 and 3 (see Fig. 6, period 2 and 3 rows, yellow boxes). However, the loss of accuracy in periods 2 and 3 is not equal for all models. The EGP 3 and EGP 2 models lead to the most significant errors in the second part (when glucagon is acting) when they are forced to fit the first part, suggesting that their structure cannot adequately describe the observed glucagon behavior.

Method C. This method aimed to reduce the differences in error between visits L and H by incorporating a variable parameter in each EGP model. All models reduced the overall RMSE achieved in Method B, except for the EGP 3 model (see Method C in Fig. 5). Hence, associating a gain change to describe differences in carbohydrate content is only effective for some models, such as the receptors or EGP 1 approach. However, a better representation of the dynamics might involve some nonlinear relationships (i.e., the behavior of glucose response is relatively similar in Period 2 both in visit L and H but presents a more acute response in the case of visit H).

Fig. 7 illustrates how the parameters changed depending on the diet. More than two-thirds of parameters (29 out of 40) increased their value to fit the greater glucagon doses. This increase was expected since the selected values would directly affect glucose values, which were higher in the HCD setting.

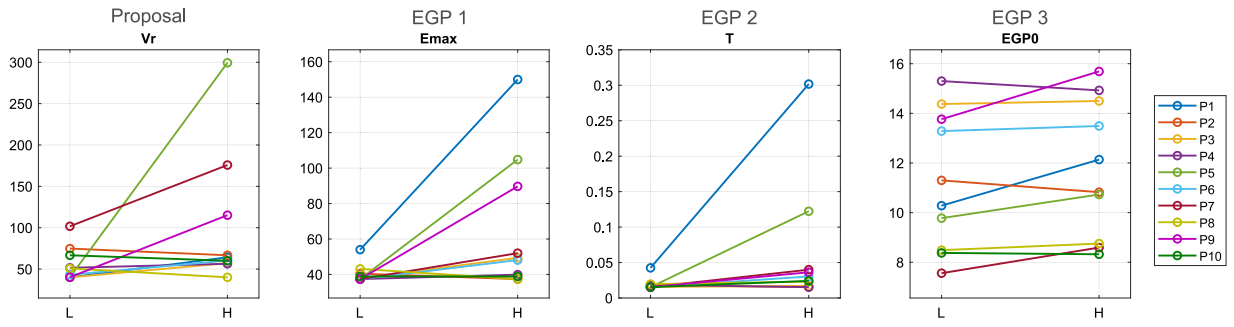

Fig. 7. Parameter variation between the identification of visit L and visit H in Method C. These parameters represent an approximation of the effect of the diet carbohydrate content on glucagon effectivity. Vertical axes represent the parameter value. Each line represents a virtual patient. The changing parameters are: V_r for the proposed EGP model (left graph), E_{max} for EGP 1 (center-left graph), T for EGP 2 (center-right graph), and EGP_0 for EGP 3 (right graph).

Fig. 7 also shows that EGP 3 experiences the most minor changes in its corresponding varying parameter, which would explain why its fit did not improve after adding the parameter change, resulting in the lowest performance in the results of Method C. Nevertheless, neither of the identification processes used favored one model over the others.

Remark that explaining diet variations with a single parameter change in the EGP definition is just an approximation to test whether this approach would improve the fit. To properly capture this kind of influence on physiology, a meal model would be needed, as well as defining a relationship between meal content and the glucagon effect model parameters. However, this proof-of-concept may serve as a baseline in future works.

Beyond the fitting accuracy, an advantage of the receptors model over the comparators is that the EGP is modeled by internal states with a physiological interpretation. Fig. 8 shows the evolution of the relative amount of receptors in each state: available ($r(t)$), active ($r_c(t)$), and internalized ($1 - r(t) - r_c(t)$). It can be observed that receptors become rapidly active the moment the glucagon is administered and then internalized, progressively recovering afterward. Since glucagon doses in this trial are sufficiently separated in time, there are sufficient available receptors when the second dose is administered. However, doses closer in time could cause a saturation in the amount of available receptors, impacting the glucagon effect on glucose, which could explain the loss of glucagon effectivity under repeated doses as observed in Blauw et al. (2016) and Bélanger et al. (2000). However, further data on glucagon receptors would be needed to research these phenomena.

Overall, both RMSE and AIC results show that the model based on glucagon dynamics achieves a better performance. The model complexity is similar to the comparators since previous studies have shown that much simpler EGP models are not able to fit glucagon dynamics (Emami et al., 2017). EGP 1 is the simplest model in this comparison and performs similarly to the proposal in some scenarios. However, the proposal still achieves a lower average AIC, with a statistically significant difference compared to EGP 1 in two of the three identification scenarios.

The authors also addressed the consideration of the model complexity, performing an additional identification. The procedure described in identification method A was replicated, including an additional simpler EGP model. The purpose was to evaluate the capacity of a simpler approach, assessing whether it could provide a similar description of the glucagon effect compared to more complex models (such as the comparators and the proposal in this work). The simpler selected model was initially presented by Smaoui et al. (2020):

$$EGP = C_p(t)S_g\mathcal{H}\left(1 - x_3(t)S_e\right) \tag{10}$$

where $C_p(t)$ and $x_3(t)$ represent the concentration of plasma glucagon and the effect of insulin on EGP, and S_g and S_e represent

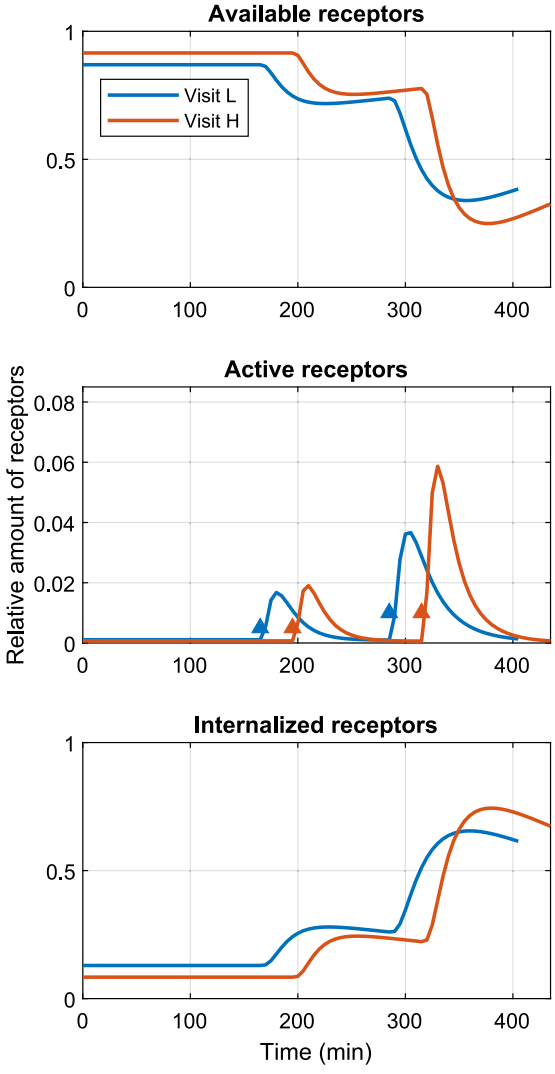

Fig. 8. Representation of the receptors states for the simulation of patient 3, for the scenario in visit L (blue lines), and visit H (orange lines). The top plot represents the relative amount of available receptors $r(t)$, middle plot shows the active receptors ($r_c(t)$), and bottom plot shows the internalized receptors ($1 - r(t) - r_c(t)$). Colored triangles represent the administration of glucagon doses (100 and 500 μg). (For interpretation of the references to color in this figure legend, the reader is referred to the web version of this article.)

glucagon and insulin sensitivity, respectively. This definition was selected because it constituted the simplest consideration that included both insulin and glucagon effect into EGP, with just two

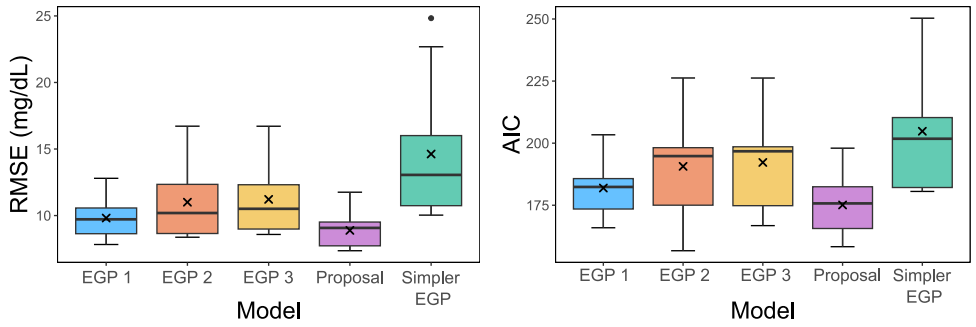

Fig. 9. RMSE (left) and AIC (right) boxplot results obtained in an identification process (following identification method A), including an additional, simpler EGP model (Smaoui et al., 2020). The outcomes were measured by simulating each model in the scenario of visits L and H, and the results aggregate the ten patients in the cohort. See more details in text.

parameters to describe their sensitivities, that also conformed to the model selection criteria established in this work, mentioned in Section 2.1, that is, that the underlying model had a similar structure to Hovorka's model (Wilinska et al., 2010).

This simpler model was implemented alongside the proposal and the comparators in this work, and their parameters were identified using identification method A (see Section 2.5.1). Fig. 9 summarizes the results obtained regarding RMSE and AIC. Even with the reduced number of parameters, which is accounted for in the calculation of the AIC, the simpler model presents significantly worse results than the other options. Moreover, the statistical analysis showed that the difference between the proposal and the simpler EGP model was statistically significant both for the RMSE and AIC (p-value of 0.002 and <0.001, respectively, and Cohen's d values were 1.38 and 1.79).

Lastly, although the presented methodology provides an evaluation of the receptors-based glucagon model, some limitations exists. First, the reduced number of patients in the dataset ($N = 10$) allows for drawing some conclusions, but a more extended cohort would allow for a more complete validation. Also, data on different settings with glucagon would be needed to validate further the model capabilities (e.g., administration of glucagon doses closer in time).

Future work may include the exploration of nonlinearities in glucagon PK observed with bigger doses. The models describing the kinetics of the small doses typically administered in AP systems may not capture the kinetics of bigger doses such as the ones used in emergency hypoglycemia rescues (typically 1 mg glucagon), leading to a misestimation of the dose effect in the simulation. Also, other datasets will be needed to assess glucagon interactions with insulin and other drugs potentially used in adjunctive therapies.

5. Conclusions

This work complements the results in Furió-Novejarque, Sanz et al. (2023) by validating an EGP definition based on glucagon receptors with a dataset with consecutive glucagon doses (100 and 500 μg) in two different diet settings (LCD and HCD). Three identification methods are presented to identify the proposed model parameters. In addition, the proposed model performance is compared to three EGP models from the literature. The proposed EGP and the comparators share the parameters of the PK/PD model used as the baseline. Results show how the proposed EGP model outperforms the comparators, providing a lower RMSE, hence performing an appropriate description of glycogenolysis and gluconeogenesis since the model describes glucose dynamics observed in clinical data.

The proposed model allows for incorporating a not-too-complex, more physiologically accurate description of glucagon into the current T1D simulators. It is, however, more complex than other proposals from the literature that achieve a similar performance level (e.g., the EGP 1 model) and could present some issues if used in model-based control algorithms. Nevertheless, focusing on using the model for simulation, the proposed EGP introduces new dynamics that have shown significant improvements in describing clinical data, paving the way to improve *in silico* validations of AP systems.

Funding

This work was partially supported by : PID2019-107722RB-C21 funded by MCIN/AEI/10.13039/501100011033, and Grant CIPROM/2021/012 funded by Conselleria de Innovación, Universidades, Ciencia y Sociedad Digital from Generalitat Valenciana, Spain. Funding for open access charge: CRUE-Universitat Politècnica de València.

CRediT authorship contribution statement

Clara Furió-Novejarque: Writing – review & editing, Writing – original draft, Visualization, Software, Methodology. **Iván Sala-Mira:** Writing – review & editing, Writing – original draft, Methodology, Investigation. **Ajenthen G. Ranjan:** Writing – review & editing, Resources. **Kirsten Nørgaard:** Writing – review & editing, Resources. **José-Luis Díez:** Writing – review & editing, Supervision. **John Bagterp Jørgensen:** Writing – review & editing, Resources. **Jorge Bondia:** Writing – review & editing, Supervision, Funding acquisition, Conceptualization.

Declaration of competing interest

The authors declare that they have no known competing financial interests or personal relationships that could have appeared to influence the work reported in this paper.

Data availability

The data that has been used is confidential.

Appendix. Parameter results and models description

This appendix includes two tables listing the units and descriptions of the base model (Table A.7) and the EGP definitions (Table A.8).

Table A.9 summarizes the identified parameters for the insulin and glucagon PK submodels. Table A.10 presents the average parameters identified with each of the methods for the PD submodel and each of the EGP definitions.

Table A.7
Baseline model states and parameters' units and description.

	Magnitude	Units	Description
Insulin PK	$u_I(t)$	U/min	Insulin infusion (as a deviation from basal)
	$X_1(t)$	U	Insulin mass due to exogenous dosing in subcutaneous tissue
	$X_2(t)$	U	Insulin mass due to exogenous dosing in plasma
	$I(t)$	mU/L	Insulin plasma concentration
	t_{max}	min	Time from dose to maximum plasma concentration
	W	kg	Weight
	$Cl_{F,I}$	mL/kg/min	Apparent insulin clearance
	I_b	mU/L	Basal insulin concentration
Glucagon PK	$u_C(t)$	pg/min	Glucagon infusion (as a deviation from basal)
	$Z_1(t)$	pg	Glucagon mass due to exogenous dosing in subcutaneous tissue
	$Z_2(t)$	pg	Glucagon mass due to exogenous dosing in plasma
	$C(t)$	pg/mL	Glucagon concentration in plasma
	k_1, k_2	min^{-1}	Absorption elimination rate constants
	$Cl_{F,C}$	mL/kg/min	Apparent glucagon clearance
	C_b	pg/mL	Basal glucagon concentration
PD	$x_1(t)$	mU/L	Effect of insulin on glucose distribution
	$x_2(t)$	mU/L	Effect of insulin on glucose disposal
	$x_3(t)$	mU/L	Effect of insulin on endogenous glucose production
	$EGP(t)$	μmol/kg/min	Endogenous glucose production
	$Q_1(t)$	μmol/kg	Glucose mass in the accessible compartment
	$Q_2(t)$	μmol/kg	Glucose mass in the non-accessible compartment
	$G(t)$	mmol/L	Blood glucose
	k_{a1}, k_{a2}, k_{a3}	min^{-1}	Deactivation rate constants
	F_{01}	μmol/kg/min	Insulin-independent glucose flux
	F_R	μmol/kg/min	Renal glucose clearance
	S_T	min^{-1}/(mU/L)	Insulin sensitivity to glucose transport
	S_D	min^{-1}/(mU/L)	Insulin sensitivity to glucose disposal
	k_{12}	min^{-1}	Transfer rate constant from the nonaccessible to the accessible compartment
	V	mL/kg	Glucose distribution volume

Table A.8
EGP models states and parameters' units and description.

	Magnitude	Units	Description
Proposed EGP	$r(t), r_C(t)$	unitless	Normalized amount of free and bonded receptors
	$F_{hgp}(t)$	μmol/kg/min	Hepatic glucose production
	k_{off}	min^{-1}	Dissociation rate
	k_{rec}	min^{-1}	Recycling rate
	k_{in}	min^{-1}	Internalization rate of the glucagon-bonded receptor
	k_{on}	$(\text{pg/min})^{-1}$	Association rate of glucagon to the receptor
	V_h	mL	Volume of the hepatic interstitial space
	K_r	unitless	Apparent dissociation constant
	V_r	μmol/kg/min	Maximal glucagon-dependent hepatic glucose production rate
	EGP_0	μmol/kg/min	EGP extrapolated to zero insulin concentration
	S_I	$(\text{mU/L})^{-1}$	Hepatic insulin sensitivity
EGP 1	$G_{gg}(t)$	μmol/kg/min	Glucose production due to glycogenolysis
	S_E	$(\text{mU/L})^{-1}$	Hepatic insulin sensitivity
	E_{max}	μmol/kg/min	Maximum EGP at basal insulin concentration
	C_{E50}	pg/mL	Glucagon concentration yielding half of maximum EGP
	G_{GNG}	μmol/kg/min	Glucose production by gluconeogenesis
EGP 2	$EGP_G(t)$	μmol/kg/min	Contribution to EGP from the rate of change of glucagon
	T_{Gd}	μmol/kg	Glucagon rate of change sensitivity
	S	$(\text{mU/L})^{-1}$	Insulin sensitivity
	T	$(\text{pg/mL})^{-1}$	Glucagon sensitivity
	G_{ng}	μmol/kg/min	Effect due to gluconeogenesis
	K_{Gd}	$(\mu\text{mol/kg})^{-1}$	Fractional deactivation rate constant
EGP 3	$Y(t)$	unitless	Effect of glucagon on EGP
	EGP_0	μmol/kg/min	Basal endogenous glucose production at zero insulin concentration
	S_f	$(\text{mU/L})^{-1}$	
	k_{g3}	min	Glucagon rate of change sensitivity
	k_c	$(\text{ng/L})^{-1}$/min	Glucagon sensitivity
	k_d	min^{-1}	Clearance rate of glucagon from the remote compartment

Table A.9
Insulin and glucagon PK parameters summary for the ten patients in the cohort for the three identification methods (A, B, C). Values are expressed as mean ± standard deviation. The values of k_2 were adjusted per visit (L or H) and per dose (100 or 500 μg). $Cl_{F,C}$ was kept the same for the first dose regardless of the visit, but it was also adjusted for the 500 μg dose. The value of k_1 was just identified per patient.

Parameter	Units	Value (mean ± SD)
t_{max}	min	73.5 ± 17.1
$Cl_{F,I}$	mL/kg/min	17.2 ± 7.8
$k_1 \cdot 10^{-4}$	min^{-1}	483 ± 140
$k_{2L\text{-}100} \cdot 10^{-2}$	min^{-1}	17.39 ± 13.55
$k_{2L\text{-}500} \cdot 10^{-2}$	min^{-1}	11.04 ± 7.77
$k_{2H\text{-}100} \cdot 10^{-2}$	min^{-1}	19.06 ± 17.09
$k_{2H\text{-}500} \cdot 10^{-2}$	min^{-1}	8.73 ± 5.27
$Cl_{F,C\text{-}100}$	mL/kg/min	91.11 ± 22.96
$Cl_{F,C\ L\text{-}500}$	mL/kg/min	57.37 ± 13.34
$Cl_{F,C\ H\text{-}500}$	mL/kg/min	66.32 ± 18.02

Table A.10
EGP models' and baseline PD parameter values summary for the ten patients in the cohort for the three identification methods (A, B, C). Values are expressed as mean ± standard deviation. Parameters V_r, E_{max}, T, and EGP_0 were adjusted per visit (L, H) in method C. Parameters S_T and S_D were adjusted per visit in every method.

Model	Parameters	Units	Method A	Method B	Method C	
Baseline PD	F_{01}	μmol/kg/min	8.9 ± 5.2	9.3 ± 4.5	9.1 ± 4.2	
	$k_{12} \cdot 10^{-4}$	min^{-1}	255 ± 181	446 ± 216	464 ± 212	
	$k_{a1} \cdot 10^{-4}$	min^{-1}	17.8 ± 13.1	49.6 ± 27.3	54.5 ± 21.8	
	$S_T \cdot 10^{-4}$	min^{-1}/(mU/L)	64.5 ± 51.2	30.3 ± 12.2	28.6 ± 11.8	L
			20.8 ± 19.2	18.3 ± 19.9	19.9 ± 15.3	H
	$S_D \cdot 10^{-4}$	min^{-1}/(mU/L)	519.9 ± 1582.3	24.0 ± 21.4	24.7 ± 25.6	
Receptors	$k_{on} \cdot 10^{-6}$	$(pg/min)^{-1}$	9.5 ± 12.0	23.9 ± 18.6	24.7 ± 11.5	
	V_r	μmol/kg/min	71.1 ± 40.1	122.5 ± 99.4	54.9 ± 20.5	L
					99.5 ± 80.7	H
	$K_r \cdot 10^{-3}$	unitless	16.2 ± 14.2	100.6 ± 120.5	64.8 ± 65.2	
	$S_I \cdot 10^{-3}$	$(mU/L)^{-1}$	23.4 ± 25.7	12.4 ± 10.2	19.3 ± 19.0	
	EGP_0	μmol/kg/min	10.8 ± 4.4	12.9 ± 2.8	12.0 ± 3.0	
EGP 1	E_{max}	μmol/kg/min	60.8 ± 23.2	46.4 ± 14.5	40.1 ± 5.2	L
					64.7 ± 37.9	H
	C_{E50}	pg/mL	1104.0 ± 516.5	819.7 ± 569.1	605.2 ± 504.4	
	$S_e \cdot 10^{-4}$	$(mU/L)^{-1}$	16.7 ± 32.3	89.8 ± 129.8	174.9 ± 146.1	
	G_{GNG}	μmol/kg/min	8.3 ± 4.7	10.7 ± 2.2	9.9 ± 2.4	
EGP 2	$T \cdot 10^{-2}$	$(pg/mL)^{-1}$	2.2 ± 0.8	2.0 ± 1.1	1.9 ± 0.8	L
					6.3 ± 9.0	H
	$K_{Gd} \cdot 10^{-2}$	$(\mu mol/kg)^{-1}$	3.5 ± 4.3	81.0 ± 246.1	74.2 ± 232.2	
	$T_{Gd} \cdot 10^{-2}$	μmol/kg	52.3 ± 31.5	72.5 ± 22.8	69.2 ± 23.6	
	$S \cdot 10^{-3}$	$(mU/L)^{-1}$	10.6 ± 11.3	11.7 ± 10.6	21.9 ± 16.6	
	G_{ng}	μmol/kg/min	10.5 ± 4.3	11.6 ± 2.6	11.4 ± 2.8	
EGP 3	$k_{g3} \cdot 10^{-6}$	min	9.1 ± 0.5	9.0 ± 0.1	9.1 ± 0.0	
	k_d	min^{-1}	0.7 ± 0.5	1.1 ± 0.6	1.0 ± 0.6	
	$k_c \cdot 10^{-3}$	$(ng/L)^{-1}$/min	1.0 ± 0.8	1.2 ± 0.5	1.2 ± 0.6	
	$S_f \cdot 10^{-6}$	$(mU/L)^{-1}$	20.1 ± 12.1	113.6 ± 51.1	97.4 ± 58.7	
	EGP_0	μmol/kg/min	10.6 ± 4.3	11.7 ± 2.6	11.3 ± 2.8	L
					11.8 ± 2.8	H

References

Ajmera, I., Swat, M., Laibe, C., Novére, N. L., & Chelliah, V. (2013). The impact of mathematical modeling on the understanding of diabetes and related complications. *CPT: Pharmacometrics and Systems Pharmacology*, *2*(7), http://dx.doi.org/10.1038/psp.2013.30.

Avgerinos, I., Manolopoulos, A., Michailidis, T., Kitsios, K., Liakos, A., Karagiannis, T., Dimitrakopoulos, K., Matthews, D. R., Tsapas, A., & Bekiari, E. (2021). Comparative efficacy and safety of glucose-lowering drugs as adjunctive therapy for adults with type 1 diabetes: A systematic review and network meta-analysis. *Diabetes, Obesity and Metabolism*, *23*(3), 822–831. http://dx.doi.org/10.1111/dom.14291.

Balsa-Canto, E., Alonso, A. A., & Banga, J. R. (2010). An iterative identification procedure for dynamic modeling of biochemical networks. *BMC Systems Biology*, *4*, http://dx.doi.org/10.1186/1752-0509-4-11.

Balsa-Canto, E., Henriques, D., Gábor, A., & Banga, J. R. (2016). AMIGO2, a toolbox for dynamic modeling, optimization and control in systems biology. *Bioinformatics*, *32*(21), 3357–3359. http://dx.doi.org/10.1093/bioinformatics/btw411.

Bélanger, P., Couturier, K., Latour, M. G., & Lavoie, J. M. (2000). Effects of supranormal liver glycogen content on hyperglucagonemia-induced liver glycogen breakdown. *European Journal of Applied Physiology*, *83*(4–5), 328–335. http://dx.doi.org/10.1007/s004210000286.

Benam, K. D., Khoshamadi, H., Åm, M. K., Stavdahl, Ø., Gros, S., & Fougner, A. L. (2023). Identifiable prediction animal model for the bi-hormonal intraperitoneal artificial pancreas. *Journal of Process Control*, *121*, 13–29. http://dx.doi.org/10.1016/j.jprocont.2022.11.008.

Bergman, R. N. (2005). Minimal model: Perspective from 2005. *Hormone Research in Paediatrics*, *64*(Suppl. 3), 8–15. http://dx.doi.org/10.1159/000089312.

Blauw, H., Joannet Onvlee, A., Klaassen, M., van Bon, A. C., & Hans Devries, J. (2021). Fully closed loop glucose control with a bihormonal artificial pancreas in adults with type 1 Diabetes: An Outpatient, Randomized, Crossover Trial. *Diabetes Care*, *44*(3), 836–838. http://dx.doi.org/10.2337/DC20-2106.

Blauw, H., Wendl, I., DeVries, J. H., Heise, T., & Jax, T. (2016). Pharmacokinetics and pharmacodynamics of various glucagon dosages at different blood glucose levels. *Diabetes, Obesity and Metabolism*, *18*(1), 34–39. http://dx.doi.org/10.1111/dom.12571.

Böhm, S. K., Grady, E. F., & Bunnett, N. W. (1997). Regulatory mechanisms that modulate signalling by G-protein-coupled receptors. *Biochemical Journal*, *322*(1), 1–18. http://dx.doi.org/10.1042/bj3220001.

Brun, R., Reichert, P., & Künsch, H. R. (2001). Practical identifiability analysis of large environmental simulation models. *Water Resources Research*, *37*, 1015–1030. http://dx.doi.org/10.1029/2000WR900350.

Castle, J. R., Youssef, J. E., Bakhtiani, P. A., Cai, Y., Stobbe, J. M., Branigan, D., Ramsey, K., Jacobs, P., Reddy, R., Woods, M., & Ward, W. K. (2015). Effect of repeated glucagon doses on hepatic glycogen in type 1 Diabetes: Implications for a bihormonal Closed-loop system. *Diabetes Care*, *38*(11), 2115–2119. http://dx.doi.org/10.2337/dc15-0754.

Dalla Man, C., Micheletto, F., Lv, D., Breton, M., Kovatchev, B., & Cobelli, C. (2014). The UVA/PADOVA type 1 diabetes simulator: New features. *Journal of Diabetes Science and Technology*, *8*(1), 26–34. http://dx.doi.org/10.1177/1932296813514502.

El Youssef, J., Castle, J. R., Bakhtiani, P. A., Haidar, A., Branigan, D. L., Breen, M., & Ward, W. K. (2014). Quantification of the glycemic response to microdoses of subcutaneous glucagon at varying insulin levels. *Diabetes Care*, *37*(11), 3054–3060. http://dx.doi.org/10.2337/dc14-0803.

Emami, A., Youssef, J. E., Rabasa-Lhoret, R., Pineau, J., Castle, J. R., & Haidar, A. (2017). Modeling glucagon action in patients with type 1 Diabetes. *IEEE Journal of Biomedical and Health Informatics*, *21*(4), 1163–1171. http://dx.doi.org/10.1109/JBHI.2016.2593630.

Faggionato, E., Laurenti, M. C., Vella, A., & Man, C. D. (2023). Nonlinear mixed effects modeling of glucagon kinetics in healthy subjects. *IEEE Transactions on Biomedical Engineering*, *70*(9), 2733–2740. http://dx.doi.org/10.1109/TBME.2023.3262974.

Furió-Novejarque, C., Sala-Mira, I., Díez, J.-L., & Bondia, J. (2024). A model of subcutaneous pramlintide pharmacokinetics and its effect on gastric emptying: Proof-of-concept based on populational data. *Computer Methods and Programs in Biomedicine*, *244*(February 2024), Article 107968. http://dx.doi.org/10.1016/j.cmpb.2023.107968.

Furió-Novejarque, C., Sala-Mira, I., Ranjan, A. G., Nørgaard, K., Díez, J.-L., Jørgensen, J. B., & Bondia, J. (2023). Validation of a model of glucagon action including glucagon receptor dynamics under consecutive doses in low and high-carb diets. *IFAC-PapersOnLine*, *56*(2), 9666–9671. http://dx.doi.org/10.1016/j.ifacol.2023.10.275.

Furió-Novejarque, C., Sanz, R., Ritschel, T. K., Reenberg, A. T., Ranjan, A. G., Nørgaard, K., Díez, J. L., Jørgensen, J. B., & Bondia, J. (2023). Modeling the effect of glucagon on endogenous glucose production in type 1 diabetes: On the role of glucagon receptor dynamics. *Computers in Biology and Medicine*, *154*, Article 106605. http://dx.doi.org/10.1016/J.COMPBIOMED.2023.106605.

Garcia-Tirado, J., Zuluaga-Bedoya, C., & Breton, M. D. (2018). Identifiability analysis of three control-oriented models for use in artificial pancreas systems. *Journal of Diabetes Science and Technology*, *12*, 937–952. http://dx.doi.org/10.1177/1932296818788873.

Haymond, M. W., Redondo, M. J., McKay, S., Cummins, M. J., Newswanger, B., Kinzell, J., & Prestrelski, S. (2016). Nonaqueous, mini-dose glucagon for treatment of mild hypoglycemia in adults with type 1 diabetes: A dose-seeking study. *Diabetes Care*, *39*(3), 465–468. http://dx.doi.org/10.2337/dc15-2124.

Herrero, P., Georgiou, P., Oliver, N., Reddy, M., Johnston, D., & Toumazou, C. (2013). A composite model of Glucagon–Glucose dynamics for in silico testing of bihormonal glucose controllers. *Journal of Diabetes Science and Technology*, *7*(4), 941–951. http://dx.doi.org/10.1177/193229681300700416.

Hinshaw, L., Mallad, A., Man, C. D., Basu, R., Cobelli, C., Carter, R. E., Kudva, Y. C., & Basu, A. (2015). Glucagon sensitivity and clearance in type 1 diabetes: Insights from in vivo and in silico experiments. *American Journal of Physiology - Endocrinology and Metabolism*, *309*(5), E474–E486. http://dx.doi.org/10.1152/ajpendo.00236.2015.

Jacobs, P. G., Resalat, N., Youssef, J. E., Reddy, R., Branigan, D., Preiser, N., Condon, J., & Castle, J. (2015). Incorporating an exercise detection, grading, and hormone dosing algorithm into the artificial pancreas using accelerometry and heart rate. *Journal of Diabetes Science and Technology*, *9*(6), 1175–1184. http://dx.doi.org/10.1177/1932296815609371.

Kelly, R. A., Fitches, M. J., Webb, S. D., Pop, S. R., & Chidlow, S. J. (2019). Modelling the effects of glucagon during glucose tolerance testing. *Theoretical Biology and Medical Modelling*, *16*(1), 1–17. http://dx.doi.org/10.1186/s12976-019-0115-3.

Koenig, J. A. (2004). Assessment of receptor internalization and recycling. *Methods in Molecular Biology (Clifton, N.J.), 259*, 249–273. http://dx.doi.org/10.1385/1-59259-754-8:249.

Lakshman, R., Boughton, C., & Hovorka, R. (2023). The changing landscape of automated insulin delivery in the management of type 1 diabetes. *Endocrine Connections*, http://dx.doi.org/10.1530/ec-23-0132.

Laugesen, C., Ranjan, A. G., Schmidt, S., & Nørgaard, K. (2023). Pen-administered low-dose dasiglucagon vs usual care for prevention and treatment of non-severe hypoglycaemia in people with type 1 diabetes during free-living conditions: a Phase II, randomised, open-label, two-period crossover trial. *Diabetologia*, *66*(7), 1208–1217. http://dx.doi.org/10.1007/s00125-023-05909-4.

Masroor, S., van Dongen, M. G., Alvarez-Jimenez, R., Burggraaf, K., Peletier, L. A., & Peletier, M. A. (2019). Mathematical modeling of the glucagon challenge test. *Journal of Pharmacokinetics and Pharmacodynamics*, *46*(6), 553–564. http://dx.doi.org/10.1007/s10928-019-09655-2.

McGough, J. J., & Faraone, S. V. (2009). Estimating the size of treatment effects: moving beyond p values. *Psychiatry (Edgmont (Pa. : Township)), 6*(10), 21–29.

McKay, M. D., Beckman, R. J., & Conover, W. J. (2000). A comparison of three methods for selecting values of input variables in the analysis of output from a computer code. *Technometrics*, [ISSN: 15372723] *42*(1), 55–61. http://dx.doi.org/10.1080/00401706.2000.10485979.

Müller, T. D., Finan, B., Clemmensen, C., Di Marchi, R. D., & Tschöp, M. H. (2017). The new biology and pharmacology of glucagon. *Physiological Reviews*, *97*(2), 721–766. http://dx.doi.org/10.1152/physrev.00025.2016.

Ramkissoon, C. M., Aufderheide, B., Bequette, B. W., & Palerm, C. C. (2014). A model of glucose-insulin-pramlintide pharmacokinetics and pharmacodynamics in type I diabetes. *Journal of Diabetes Science and Technology*, *8*(3), 529–542. http://dx.doi.org/10.1177/1932296813517323.

Ranjan, A., Schmidt, S., Damm-Frydenberg, C., Steineck, I., Clausen, T. R., Holst, J. J., Madsbad, S., & Nørgaard, K. (2017). Low-carbohydrate diet impairs the effect of glucagon in the treatment of insulin-induced mild hypoglycemia: A randomized crossover study. *Diabetes Care*, *40*(1), 132–135. http://dx.doi.org/10.2337/dc16-1472.

Ranjan, A., Schmidt, S., Madsbad, S., Holst, J. J., & Nørgaard, K. (2016). Effects of subcutaneous, low-dose glucagon on insulin-induced mild hypoglycaemia in patients with insulin pump treated type 1 diabetes. *Diabetes, Obesity and Metabolism*, *18*(4), 410–418. http://dx.doi.org/10.1111/dom.12627.

Resalat, N., Youssef, J. E., Tyler, N., Castle, J., & Jacobs, P. G. (2019). A statistical virtual patient population for the glucoregulatory system in type 1 diabetes with integrated exercise model. *PLoS ONE*, *14*(7), Article e0217301. http://dx.doi.org/10.1371/journal.pone.0217301.

Rimmington, F. (2020). Pharmacokinetics and pharmacodynamics. *Southern African Journal of Anaesthesia and Analgesia*, *26*(6), S153–S156. http://dx.doi.org/10.36303/SAJAA.2020.26.6.S3.2562.

Ronald Kahn, C. (1976). Membrane receptors for hormones and neurotransmitters. *Journal of Cell Biology*, *70*(2), 261–286. http://dx.doi.org/10.1083/jcb.70.2.261.

Sedaghat, A. R., Sherman, A., & Quon, M. J. (2002). A mathematical model of metabolic insulin signaling pathways. *American Journal of Physiology - Endocrinology and Metabolism*, *283*(5), 1084–1101. http://dx.doi.org/10.1152/ajpendo.00571.2001.

Shrayyef, M. Z., & Gerich, J. E. (2010). Normal glucose homeostasis. *vol. 53*, In *Principles of diabetes mellitus* (pp. 19–35). Boston, MA: Springer US, http://dx.doi.org/10.1007/978-0-387-09841-8_2.

Smaoui, M. R., Rabasa-Lhoret, R., & Haidar, A. (2020). Development platform for artificial pancreas algorithms. In O. Moser (Ed.), *PLOS ONE*, *15*(12), Article e0243139. http://dx.doi.org/10.1371/journal.pone.0243139.

van Sloun, B., Goossens, G. H., Erdõs, B., O'Donovan, S. D., Singh-Povel, C. M., Geurts, J. M., van Riel, N. A., & Arts, I. C. (2023). E-DES-PROT: A novel computational model to describe the effects of amino acids and protein on postprandial glucose and insulin dynamics in humans. *iScience*, *26*(3), Article 106218. http://dx.doi.org/10.1016/j.isci.2023.106218.

Visentin, R., Campos-Náñez, E., Schiavon, M., Lv, D., Vettoretti, M., Breton, M., Kovatchev, B. P., Dalla Man, C., & Cobelli, C. (2018). The UVA/Padova type 1 diabetes simulator goes from single meal to single day. *Journal of Diabetes Science and Technology*, *12*(2), 273–281. http://dx.doi.org/10.1177/1932296818757747.

Wendt, S. L., Ranjan, A., Mø ller, J. K., Schmidt, S., Knudsen, C. B., Holst, J. J., Madsbad, S., Madsen, H., Nørgaard, K., & Jørgensen, J. B. (2017). Cross-validation of a Glucose-Insulin-Glucagon pharmacodynamics model for simulation using data from patients with type 1 diabetes. *Journal of Diabetes Science and Technology*, *11*(6), 1101–1111. http://dx.doi.org/10.1177/1932296817693254.

Wilinska, M. E., Chassin, L. J., Acerini, C. L., Allen, J. M., Dunger, D. B., & Hovorka, R. (2010). Simulation environment to evaluate closed-loop insulin delivery systems in type 1 diabetes. *Journal of Diabetes Science and Technology*, *4*(1), 132–144. http://dx.doi.org/10.1177/193229681000400117.

Woods, S. C., Lutz, T. A., Geary, N., & Langhans, W. (2006). Pancreatic signals controlling food intake; insulin, glucagon and amylin. *Philosophical Transactions of the Royal Society, Series B (Biological Sciences)*, *361*(1471), 1219–1235. http://dx.doi.org/10.1098/rstb.2006.1858.